21

Procedures for Evaluation of Slice Thickness in Medical Imaging Systems

Giuseppe Vermiglio, Giuseppe Acri, Barbara Testagrossa, Federica Causa and Maria Giulia Tripepi
Environmental, Health, Social and Industrial Department – University of Messina
Italy

1. Introduction

The main goal of a medical imaging system is to produce images to provide more accurate and timely diagnoses (Torfeh et al., 2007). In particular, Computed Tomography (CT), Magnetic Resonance Imaging (MRI), and Ultrasound (US) are resourceful tools in medical practice, and in many cases a life saving resource when rapid decisions are needed in the emergency room (Rehani et al., 2000). The above diagnostic techniques are based on the evaluation of high resolution images from technologically sophisticated equipment. Individual images are obtained by using several different electronic components and considerable amounts of data processing, which affect the quality of images produced and, consequently, make the diagnostic process more complicated (Torfeh et al., 2007).
In this context, to guarantee a consistent image quality over the lifetime of the diagnostic radiology equipment and to ensure safe and accurate operation of the process as a whole, it is necessary to establish and actively maintain regular and adequate Quality Assurance (QA) procedures. This is significant for computer-aided imaging systems, such as CT, MRI and US. The QA procedure should include periodic tests to ensure accurate target and critical structure localization (Mutic et al., 2003). Such tests are referred to as Quality Controls (QCs). They hold a key role within the QA procedure because they enable complete evaluation of system status and image quality (Chen et al., 2004; Vermiglio et al., 2006).
Importantly, QCs permit the identification of image quality degradation before it affects patient scans, and of the source of possible equipment malfunction, pointing to preventive or immediate maintenance requirements. Thus, image QC is crucial to ensure a safe and efficient diagnosis and treatment of diseases (Rampado et al., 2006; Torfeh et al., 2007). For this reason, periodic QCs have been recommended by manufacturers and medical physicists' organizations to test the performance of medical imaging systems. Protocols for QCs and QA in medical imaging systems have been produced by several professional groups (AAPM – NEMA) (Goodsitt et al., 1998). This highlights the extensive role of QA programs, including QC testing, preventive maintenance, etc. (Rampado et al., 2006).
In any clinical imaging study, it is important to have accurate confirmation of several physical characteristics of the medical imaging device. In particular, the slice thickness

accuracy represents an important parameter that should be estimated during QC procedures, not only because the signal to noise ratio varies linearly with the slice thickness, but also because clinical image resolution is strongly affected by partial volume effects, thus reducing clinical image quality with increasing slice thickness (Narayan et al., 2005). In addition, to determine the FWHM the AAPM procedure involves the evaluation of a line profile of the slice. So, during QC procedures many and different available test objects are used to assess different physical characteristics of the medical imaging device, including slice thickness, spatial resolution, dark noise, uniformity, etc. AAPM Reports No 1 and No 28 state that the slice thickness can be evaluated from the measure of the full width at half maximum (FWHM) of the response across the slice (Judy et al., 1977; Price et al., 1990). In particular, for a high-accuracy measurement of slice thickness, several test objects inserted in multipurpose phantoms can be used, most of which utilize inclined surfaces (plane, cone or spiral). A typical test object for the slice thickness evaluation is the crossed high signal ramps oriented at a fixed angle (Price et al., 1990).

Whereas in US equipment the slice thickness is typically not measured (Skolnick, 1991), most CT and MRI scanners adopt specific and automated procedures that require the use of dedicated phantoms, coupled with a dedicated imaging software that, however, does not always include line profile tools.

Standard slice thickness accuracy evaluation methods consist of scan explorations of phantoms that contain different specific patterns. These methods are based on manual scans with graphics tools or, alternatively, on automatic scans utilizing encoded masks to determine the Region Of Interest (ROI) for quantization (Torfeh et al., 2007). Therefore, a variety of different phantoms presently exists, but each requiring a specific QC protocol.

Further, even the newest medical imaging software do not allow a direct measurement of the slice thickness accuracy with CT and MRI scanners, but require a complicated procedure to be performed by specialized technicians authorized to enter in the SERVICE menu of medical devices.

To reduce complications and provide a versatile and unique QC procedure to estimate slice thickness accuracy, a novel dedicated phantom and associated procedure is proposed here that is easy to implement and that can be used on both CT and MRI scanners.

Such phantom can be used either with already existing dedicated software or with to this aim dedicated LabView-based tools, to readily measure the slice thickness in real time and/or post-processing operation. The reliability of the innovative technique proposed here has been evaluated with respect to previously validated procedures by conducting statistical analysis, as discussed in detail in the following sections.

Further, this novel technique is suitable also for the evaluation of the elevation resolution in US scanners, and easier to perform than standard techniques. This chapter is structured as follows: a review of the materials and methods commonly used in CT, MRI and US imaging systems, and the novel and versatile methodology proposed here for slice thickness measurements are presented in Section 2. The results obtained from the application of the proposed novel methodology to the three different imaging techniques are discussed in Section 3. The conclusions are drawn in Section 4.

2. Materials and methods

In this section the commonly used methods for determining the slice thickness accuracy in CT, MRI and US scanners are presented. In addition, a novel procedure that uses a

dedicated phantom and the following image elaboration by employing LabView based software is also proposed.

2.1 CT scanners

The slice thickness is evaluated by measuring the width (FWHM) of the image of one or more Aluminium ramps at the intersection of the ramp(s) with the scan plane (CEI, 1998), as illustrated schematically in Fig. 1. The sensitivity profile measures the system response to an attenuating impulse as a function of the z-axis position, through the slice plane. The sensitivity profile is a function of pre- and post-patient collimation, and appears as a blurred square wave. The FWHM of this blurred square is defined as the nominal slice width. The slice thickness of a CT scanner is determined by focal spot geometry as well as pre-patient and detector collimation and alignment.

An customary method of monitoring equipment performance is to measure the parameters of interest using test objects. For example, Goodenough et al. proposed an approximate measure of beam width by using a series of small beads positioned across the beam width. However, this phantom is difficult to use for a precise quantitative measure because of the uncertainty on the alignment of the beads with respect to the beam. Indeed, the beam width can be measured directly from a beam profile plot only if care is taken to ensure that the Aluminium piece is oriented at 45 degrees across the width of beam (Judy et al., 1977, as cited in Goodenough et al., 1977).

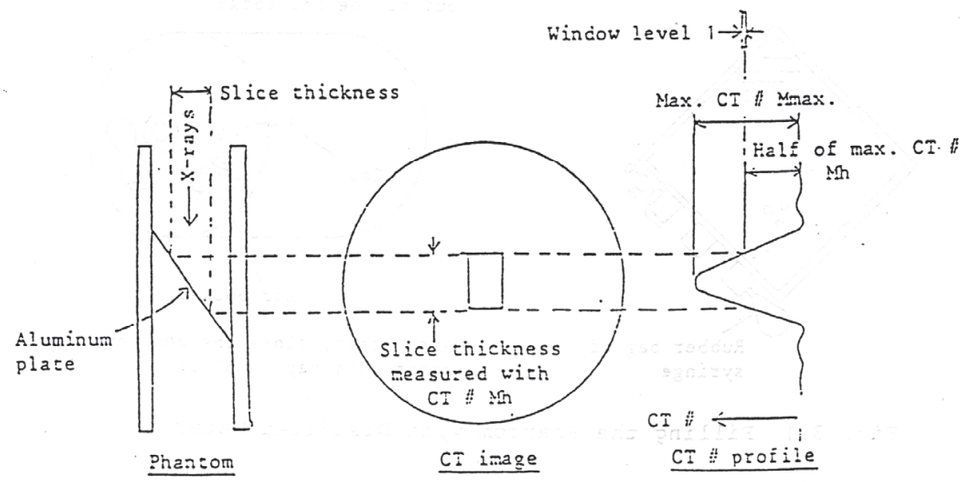

Fig. 1. Principle of slice thickness measurement (Philips, 1997).

A typical performance phantom (Philips, 1997) uses Aluminium plates slanted 26.565 degrees and which are across each other, as shown in Fig. 2. With X-rays irradiated to the Aluminium plates, the axial length of each Aluminium can be measured in CT image. With this method, it is possible to obtain an accurate measurement even if the intersection of the Aluminium plates is not aligned with the X-ray beam, by averaging the two measurements L_a and L_b. The slice thickness L is calculated as follows:

$$L = \left(\frac{L_a + L_b}{2} \right) \cdot \tan 26.565° = \frac{L_a + L_b}{4} \tag{1}$$

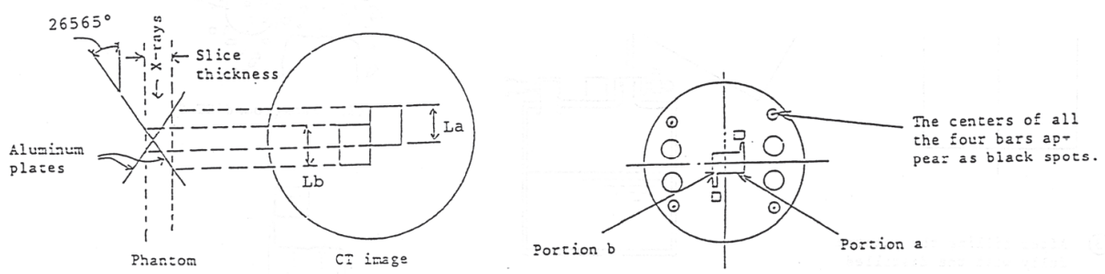

(a) (b)

Fig. 2. CT image of the section dedicated to the measurements of slice thickness of a typical performance phantom: (a) layout of the measurement methodology; (b) schematic of resulting image with the centres of the four bars appearing as black spots (Philips, 1997).

Another performance phantom used for CT scanners (Fig. 3) is a poli methyl methacrilate (PMMA) box presenting a pattern of air filled holes drilled 1 mm apart and aligned in the direction of the slice thickness (perpendicular to the scan plane). Each visible hole in the image represents 1 mm of beam thickness (General Electric [GE], 2000).

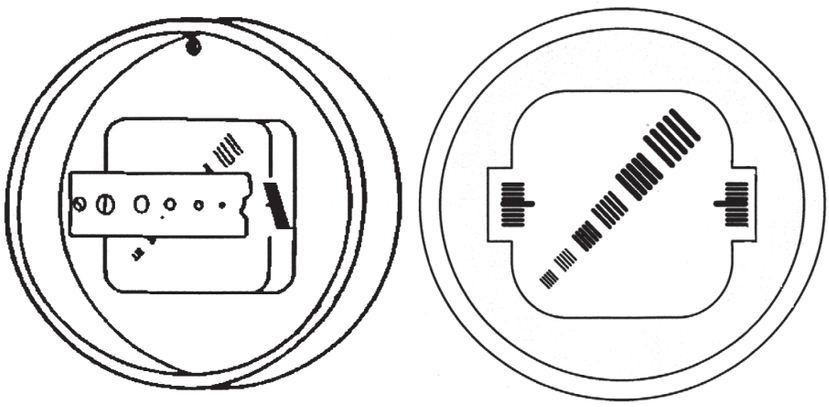

(a) (b)

Fig. 3. Phantom with air-filled holes for slice thickness measurement in CT scanners: (a) schematic of the phantom, (b) schematic of the calibration image (General Electric [GE], 2000).

To determine the slice thickness, the image is displayed at the recommended window level and width. The number of visible holes (representing air-filled holes) is counted. Holes that appear black in the image represent a full millimetre slice thickness. Holes that appear grey count as fractions of a millimetre; two equally grey holes count as a single 1 mm slice thickness.

2.2 MRI scanners

The technique of MRI differs from X-ray CT in many ways, but one of the most interesting is perhaps that the slice is not determined primarily by the geometry of the scanning apparatus but rather by electronic factors, namely the spectrum of radio frequency pulse and the nature of the slice selection gradient (Mc Robbie et al., 1986). The slice profile and width of a 2D imaging technique such as MRI is a very important feature of its performance.

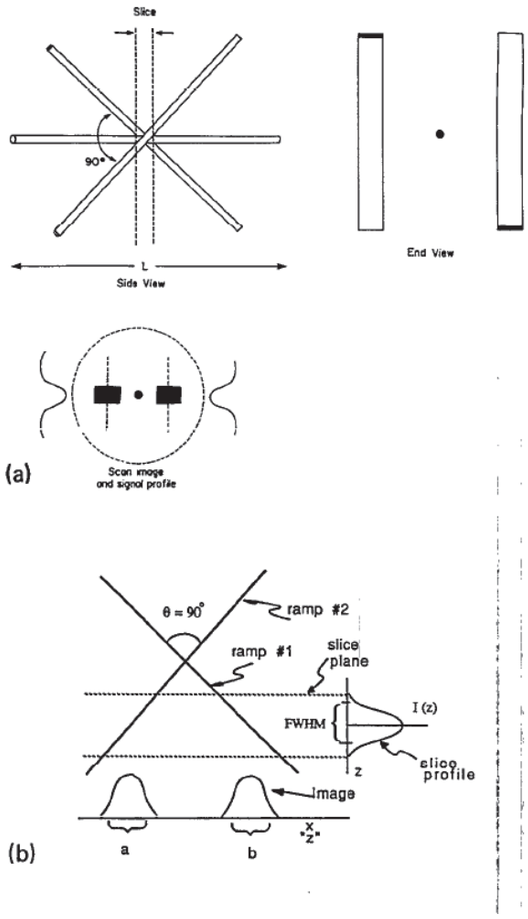

Fig. 4. High signal ramp phantoms: (a) A typical slice-thickness phantom consisting of a set of crossed thin ramps. A ramp crossing angle of 90° yields an angle of 45° between the ramp and the image plane. The phantom length (L) should be greater than twice the maximum slice thickness. An alignment rod placed between the two ramps defines the point where the two ramps cross. When the slice is properly aligned through the intersection of the ramps the images of the ramps and of the rod will be aligned. (b) The slice sensitivity profile is directly proportional to the image intensity profiles if the image plane is perpendicular to the alignment rod (Price et al., 1990).

Since the signal obtained is directly proportional to the thickness of the slice, an inaccurate slice width can lead to a reduced Signal-to-Noise Ratio (SNR) (Lerski, 1992). Partial volume effects can significantly alter sensitivity and specificity. Quantitative measurements such as relaxation time T_1 and T_2 values, are also greatly influenced by slice thickness. Inaccuracies in slice thickness may result in inter-slice interference during multi-slice acquisitions, and invalid SNR measurements (Och et al., 1992). The slice profile, ideally rectangular, may contain side lobes which can produce very confusing effects (Lerski, 1992). In addition, gradient field nonuniformity, radio frequency field nonuniformity, nonuniform static magnetic field, noncoplanar slice selection pulses between excitation and readout, T_R/T_1 ratio (where T_R represents the repetition time), and radio frequency pulse shape and stimulated echoes can also affect the slice thickness accuracy (Price et al., 1990).

A variety of phantoms have been designed to evaluate slice thickness. All are some variation of an inclined surface. These may include wedges, ramps, spirals, or steps. A typically used phantom is the crossed high signal ramps.

High signal ramp (HSR) phantoms generally consist of opposing ramp pairs oriented at a fixed angle θ (Fig. 4). The HSR's should be thin (ideally infinitesimally thin) to quantify the slice profile accurately. In general, the thickness of a (90°) HSR oriented at 45° respect to the image plane should be < 20% of the slice profile FWHM (i.e., for 5-mm slice it is necessary to use a l-mm ramp) to obtain a measurement with < 20% error.

The FWHM is the width of the slice profile (SP) at one-half of the maximum value. In this case, the SP should be obtained for each ramp. The FWHM then becomes

$$L = FWHM = \frac{(a+b)\cos\theta + \sqrt{(a+b)^2\cos^2\theta + 4ab\sin^2\theta}}{2\sin\theta} \tag{2}$$

where *a* and *b* refer to the FWHM of the intensity profiles measured for ramp 1 and ramp 2, respectively. Note that for θ=90° then Eq. 2 is simplified to:

$$L = FWHM = \sqrt{ab} \tag{3}$$

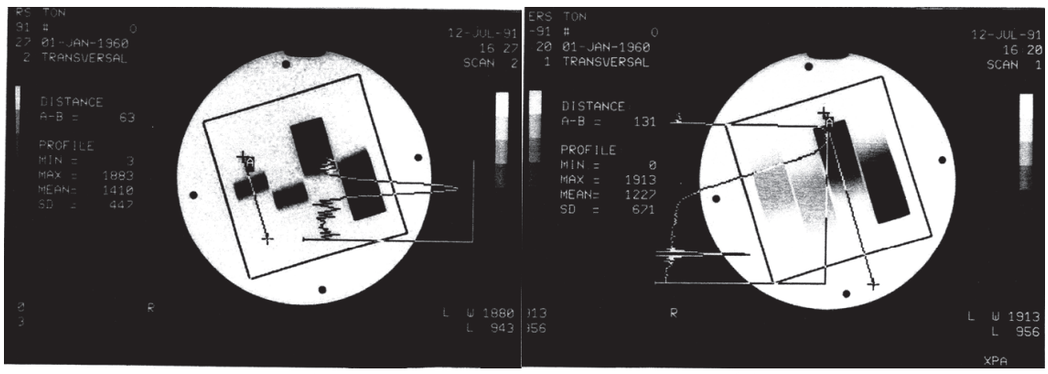

(a) (b)

Fig. 5. Example of CT scanner image obtained from the assessment of the EUROSPIN phantom (Lerski, 1992).

The EUROSPIN test phantom contains two sets of structures that may be used for slice profile and width measurement. Pairs of angled plates are used to obtain a direct measurement. The additional pairs of wedges are used to calibrate especially thin slices. Typical examples of images obtained for slice width are presented in Fig. 5(a and b). The dark bands on the left hand side of Fig. 5a represent a projection of the slice profile from the angled plates; the shaded region on the right hand side of the Fig. 5b represents the projection of the profile at the wedge.

2.3 US scanners

Ultrasound image resolution depends on beam width in the scan and elevation (section thickness) planes (Skolnick, 1991). On US scanners slice thickness evaluation or elevational resolution is useful to understand some of the problems due to partial volume effect. Section thickness is significantly more complicated to check. This characteristic of the ultrasound

beam depends on the focusing effect in the elevation direction, which is perpendicular to the scanning plane (Richard, 1999). In linear, curved linear and phased array sector probes, focus is controlled electronically, but in the elevation plane it is determined mechanically by the curvature of the crystals. The beam in the scan plane can be sharply focused only in a narrow focal range. Thus, beam profiles in the scan plane are not indicative of beam profiles in the elevation plane. As with lateral and axial resolution, elevational resolution can be measured indirectly with anechoic spherical objects or cylindrical plug phantoms. Slice thickness focusing can also be evaluated qualitatively by scanning the anechoic cylindrical objects in an ultrasound QC test phantom with the scan plane along the lengths of the cylinders (e.g., perpendicular to the usual scan direction). Quantitative assessment can be achieved by using an "inclined plane" phantom (Fig. 6) (Goodsitt et al., 1998).
The methodology used with the inclined plane phantom consists in obtaining the elevation beam profile, finding the depth where the image is narrowest. By focusing on that plane, the thickness of the image is measured at the focal plane.

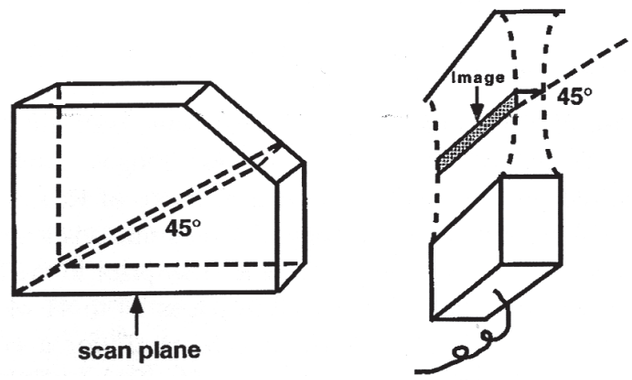

Fig. 6. Phantom used for beam width measurement in the elevation plane: (a) schematic of the phantom; (b) schematic of the procedure to obtain the image at the beam waist (Goodsitt et al., 1998).

This technique enables measurement of the elevation dimension of the beam only at a single depth. To determine the entire profile in the elevation plane, the probe must be moved horizontally along the surface of the phantom to make a series of measurements, with the beam intersecting the inclined plane at different depths (Skolnick, 1991).
Slice thickness focal range, thickness and depth should be recorded on the US unit for each commonly used transducer. Any significant variation from those reference values may indicate a detachment of the focusing lens.

2.4 The novel procedure

A novel and versatile methodology is proposed here to determine the slice thickness accuracy using a novel phantom. The methodology can be applied to any image scanning technique, including CT, MRI and US scanning. The methodology consists of two steps: 1) acquisition of images of the phantom; 2) image elaboration by using the dedicated LabView-based software. To test the proposed procedure and to obtain detailed information about the

quality of the obtained results, the acquired and processed images were compared with those obtained by elaborating the same phantom images using commercial software following already validated procedures (Testagrossa et al., 2006).
The novel proposed dedicated phantom consists of a poli-methyl-methacrilate (PMMA) empty box (14.0 cm x 7.5 cm x 7.0 cm) diagonally cut by a septum at 26 degrees (Fig. 7). The PMMA septum is 2.0 mm thick and it divides the box into two sections, thus reproducing both single and double wedges. The two sections can be filled with the same fluid or with fluids of different densities. In particular, to determine the slice thickness accuracy the PMMA box was filled with two different fluids (water and air) for assessment in a CT scanner. To perform the same assessment with an MRI scanner, water was replaced with a $CuSO_4$ $5H_2O$+H_2SO_4+1ml/l antialga (ARQUAD) liquid solution (T_1=300 ms, T_2=280ms). For US systems the upper wedge was filled with ultrasound gel, as conductive medium.
In addition, a spirit level is used to verify the planarity of the phantom with respect to the beam and the patient couch.

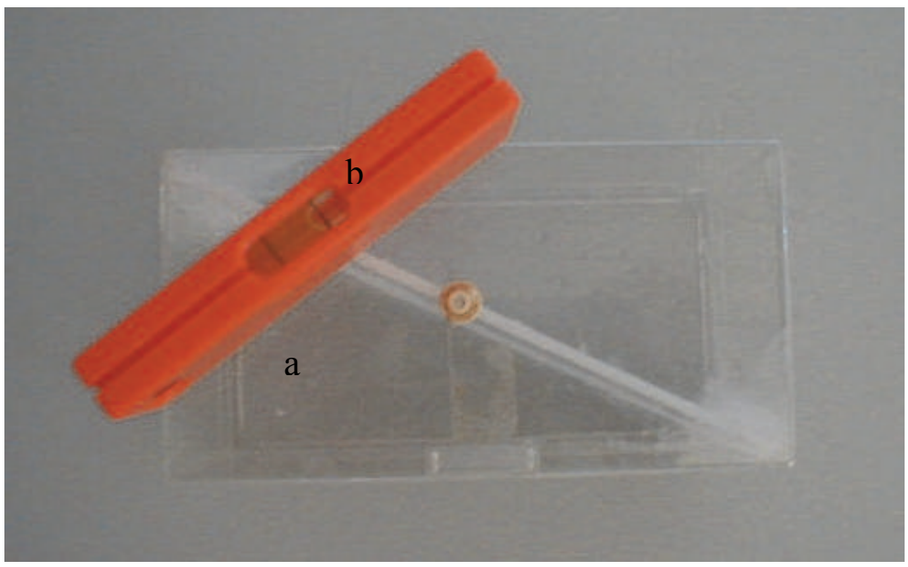

Fig. 7. The novel proposed PMMA phantom for the evaluation of the slice thickness accuracy: (a) proposed for the evaluation of the slice thickness accuracy. (b) the spirit level used to verify the planarity of the phantom with respect to the beam and the patient couch is also shown for completeness.

The test procedure followed for both CT and MRI devices consists of four steps:
1. Placing the slice thickness accuracy phantom in the scanner head holder.
2. Adjusting level position of the phantom if necessary.
3. Moving/positioning the phantom in the gantry aperture.
4. Scanning the phantom with a single slice using the desired slice width available

The phantom images were acquired using standard Head and Body protocols, shown in Table 1 and Table 2 for CT and MRI medical devices, respectively. After, the phantom images were acquired, elaborated and analyzed, they were stored and/or transmitted to a printer. The stored ones were further transferred to a dedicated workstation, whereas the printed ones were acquired by the same workstation using a VIDAR Scanner, for the next elaboration.

Scan Parameters	Head Protocol	Body Protocol
kV	120	120
mA	100	45
Scan Time (s)	3	1
Field of View (mm)	230	360
Reconstruction Matrix	512	512
Filter	None	None

Table 1. Standard Protocol for testing CT medical devices.

Scan Parameters	Head Protocol	Body Protocol
Coil type	Head	Body
Scan mode	SE	SE
Scan technique	MS	MS
Slice orientation	Transversal	Transversal
Numbers of echoes	2	3
Field of View (mm)	250	250
Repetition Time (ms)	1000	1000
Scan matrix	256	256
Water fat shift	1.3	Maximum

Table 2. Standard Protocol for testing MRI medical devices.

The methodology developed here for data elaboration, utilizes a purposely developed LabView-based slice thickness measurement software. LabView is a graphical programming language that uses icons instead of lines of text to create applications. In contrast to text-based programming languages, where instructions determine program execution, LabView uses data flow programming, where the flow of data determines execution (National Instruments [NI], 2003). The software is compatible with both non-standard and standard image formats (BMP, TIFF, JPEG, JPEG2000, PNG, and AIPD) (Vermiglio et al., 2008). To evaluate the slice width the FWHM of the wedge, expressed in pixels, is measured and calibrated with respect to the effective length of the PMMA box, expressed in mm. The result is displayed in real-time at the user interface, known as the software Front Panel (Fig. 8), with the advantage of providing a complete set of data with a user-friendly interface.
By plotting the radiation profile obtained as a system response to an attenuating impulse, as a function of position (z axis), that is through the slice plane, it is possible to estimate the slice thickness accuracy of the acquired image utilising the developed software. This is referred to as the sensitivity profile. Gaussian smoothing is applied to smooth out the sensitivity profile and permit a clearer estimate of the desired FWHM. To evaluate the slice thickness , in real time, the software utilises the following equation:

$$ST = FWHM \cdot \tan(26°) \tag{4}$$

To test the proposed procedure, results are compared with those obtained by elaborating the same phantom images using commercial software, in particular Image-Pro Plus software from Media Cybernetics (Sansotta et al., 2002; Testagrossa et al., 2006).

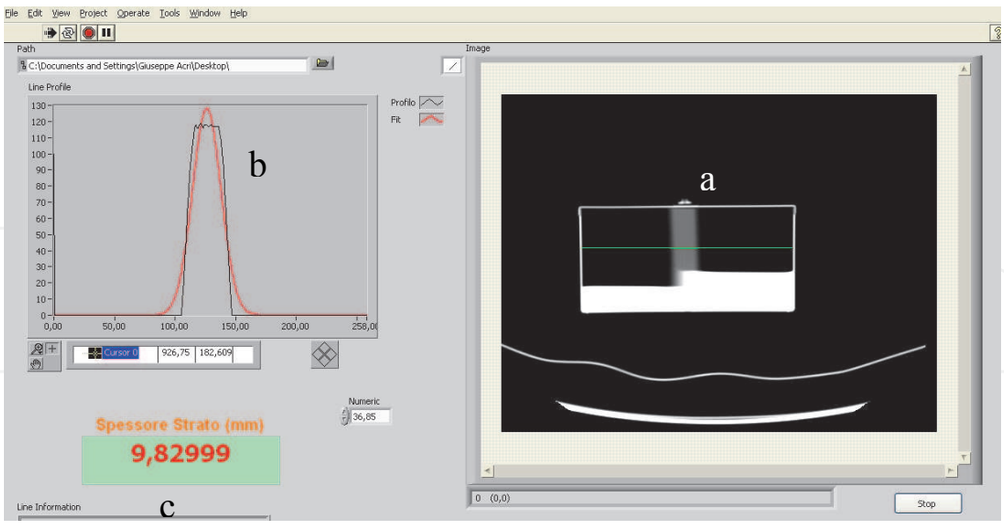

Fig. 8. Front Panel of the dedicated slice thickness LabView software showing (a) X-ray phantom section, (b) the detected line profile and corresponding Gaussian fit, and (c) the resulting slice thickness value. All steps are performed in real time.

The measurements presented here have been conducted on several CT and MRI devices in an extended study from 2006 to 2010. In addition, a statistical analysis was conducted on the resulting datasets to further validate the proposed methodology. The chosen statistical method is the variance analysis, through Fisher's exact test (F-test), to assess if a significant difference exists between datasets obtained following different procedures (C.A. Markowski & E.P. Markowski, 1990). The F-test is useful when the aim of the study is the evaluation of the precision of a measurements technique. In fact, the variance analysis consists in the factorisation of the total variance into a set of partial variances corresponding to different and estimated variations. The statistical analysis was conducted both on CT and MRI datasets.

For CT scanners three different datasets of slice thickness measurements were considered. The first dataset of 16 measurements was done on a reference (RF) value of 10 mm The second dataset of 14 measurements, on a RF value of 5 mm. The third dataset of 10 measurements, on a RF value of 2 mm. The data was obtained using two different procedures.

For MRI scanners slice thickness measurements were done on a RF value of 10 mm. In this case three different procedures were compared and 24 measurements in total were obtained on different MRI systems.

3. Results

The slice thickness measurements results using the novel proposed methodology and the statistical data analysis are presented in this section for CT, MRI and US systems.

3.1 CT medical devices

A two-dimensional image of the wedge of the dedicated phantom of Fig. 7 was acquired using the Standard Head Protocol described in Table 1. The X-Ray image of the phantom is presented in Fig. 9. In this case the line profile tool was available and the related trend was shown in the same figure.

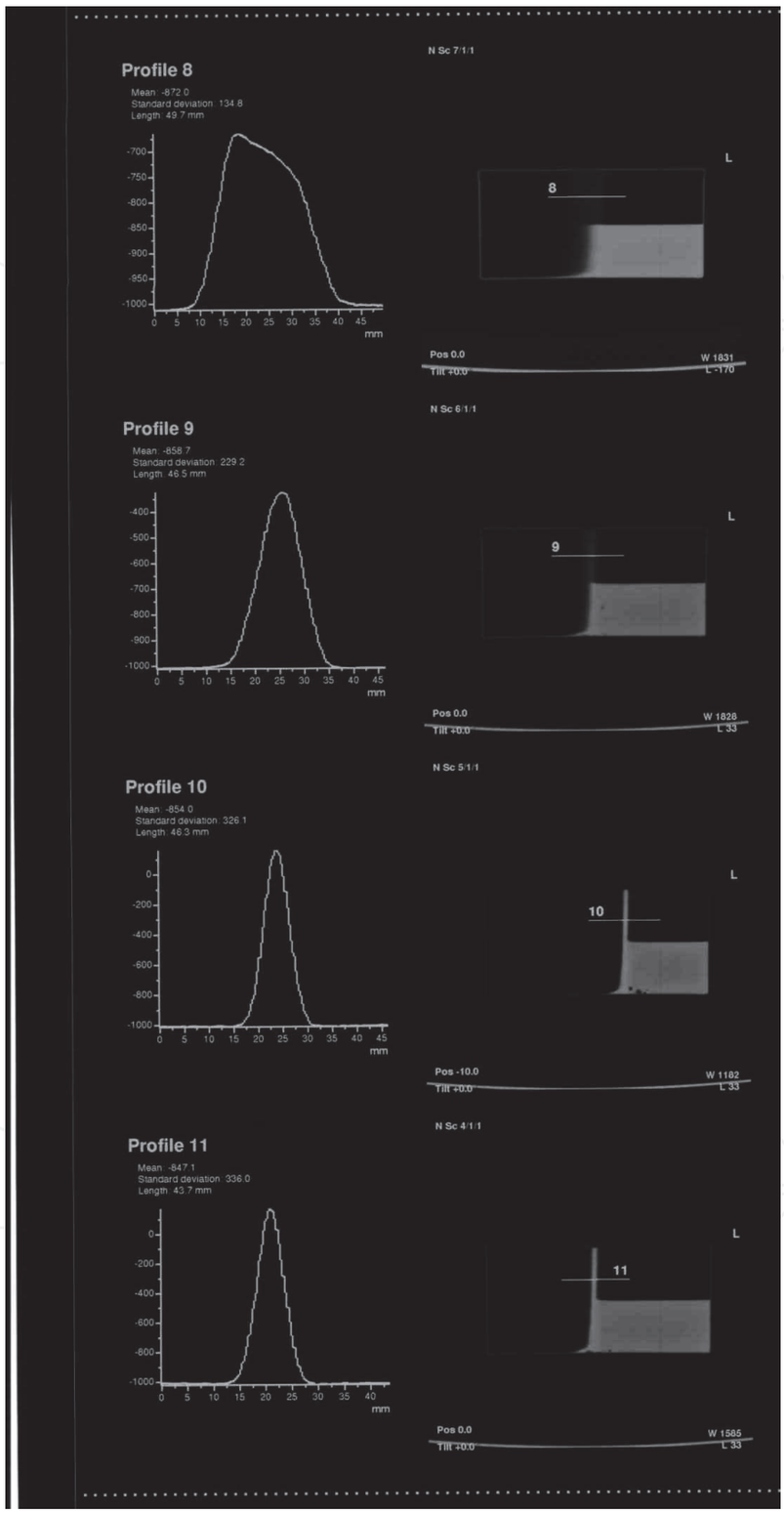

Fig. 9. CT scanner in-built software results displaying the line profiles obtained for different readings of the X-ray image of the dedicated phantom.

The results obtained by measuring the slice thickness accuracy with different CT scanners and by employing the in-house developed LabView (LV) program and the commercial Image Pro Plus (IPP) software are compared with the corresponding 10 mm RF value in Table 3. In the same table mean values and standard deviations are also reported for both procedures.

RF Value (mm)	LV (mm)	LV mean value and standard deviation (mm)	IPP (mm)	IPP mean value and standard deviation (mm)
10	8.61	9.69±0.68	8.07	9.64±1.26
	9.30		10.33	
	9.44		9.44	
	10.80		10.04	
	9.50		8.62	
	10.18		12.00	
	10.26		8.54	
	9.45		10.10	

Table 3. Slice thickness accuracy results obtained with LV and IPP for a 10 mm RF value, using different types of CT scanners.

The data of Table 3 are presented in graphical form in Fig. 10. The slice thickness accuracy results (blue: IPP; red: LV) and deviation from the RF value (blue: IPP; red: LV) obtained using the IPP and LV procedures are presented for the 10 mm RF value.

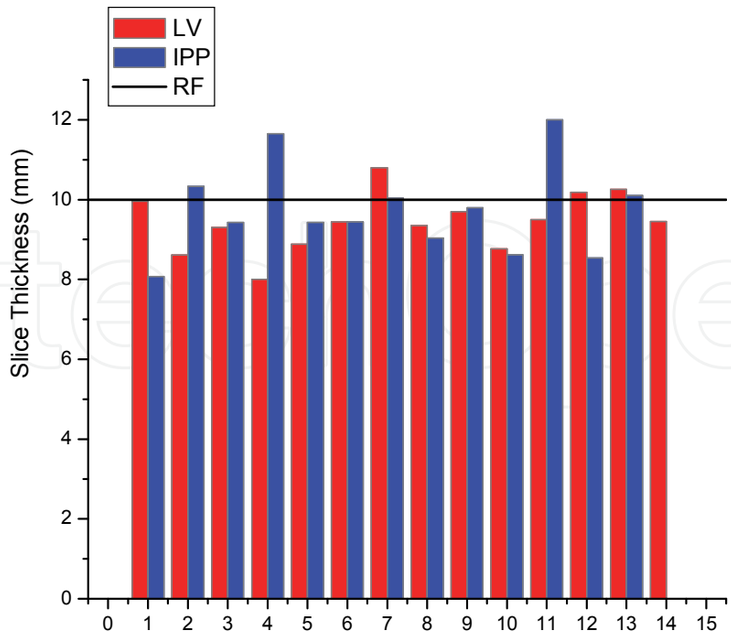

Fig. 10. (a)

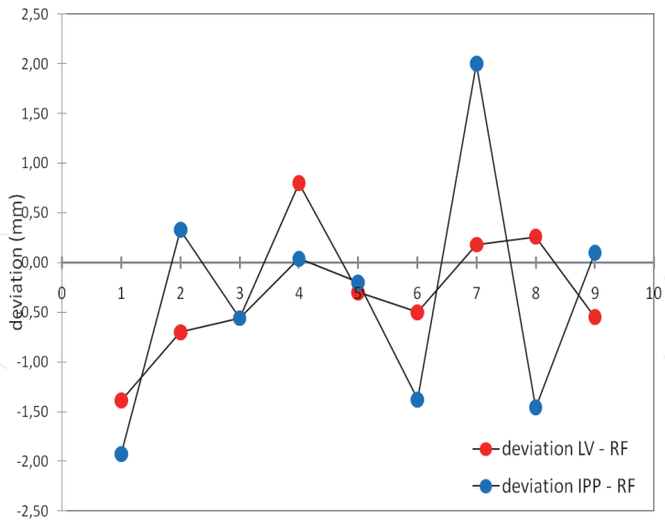

(b)

Fig. 10. CT slice thickness accuracy obtained for a 10mm RF value: (a) data set (blue: IPP; red: LV); (b) deviation from the RF value (blue: IPP; red: LV).

From the results presented in Table 3, it is observed that the mean values calculated for both the IPP and LV procedures, are comparable. However, the standard deviation obtained from the two different procedures is considerably different, with the LV procedure providing a narrower deviation, and hence more accurate results of the performed measurements.

In Table 4, the slice thickness accuracy results obtained with IPP and LV are compared with the corresponding 5 mm RF value. Also in this case, for the sake of completeness, the respective mean values and standard deviations obtained from the IPP and LV datasets are reported.

RF Values (mm)	LV (mm)	LV mean value and standard deviation (mm)	IPP (mm)	IPP mean value and standard deviation (mm)
5	4.50	4.73±0.25	4.03	4.83±0.41
	4.75		4.82	
	4.80		4.83	
	4.36		5.36	
	4.89		4.85	
	4.71		4.80	
	5.13		5.13	

Table 4. Slice thickness accuracy results obtained with LV and IPP for a 5mm RF value, using different types of CT scanners.

Also for the 5 mm RF value case, the mean values obtained from LV and IPP datasets are comparable, with a slightly better estimate for the IPP procedure. However, the standard deviations obtained from the two procedures are significantly different. As in the previous case, the LV procedure provides a narrower deviation, thus enabling a more accurate measurement.

The data of Table 4 are reported in graphical form in Fig 11, where the slice thickness accuracy results obtained with the two procedures (blue: IPP; red: LV) and their deviation from the 5 mm RF value are presented.

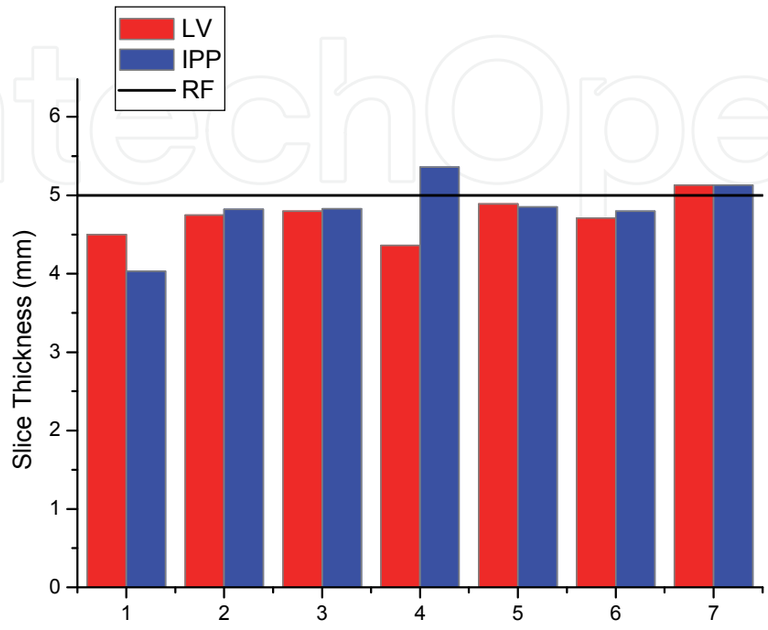

(a)

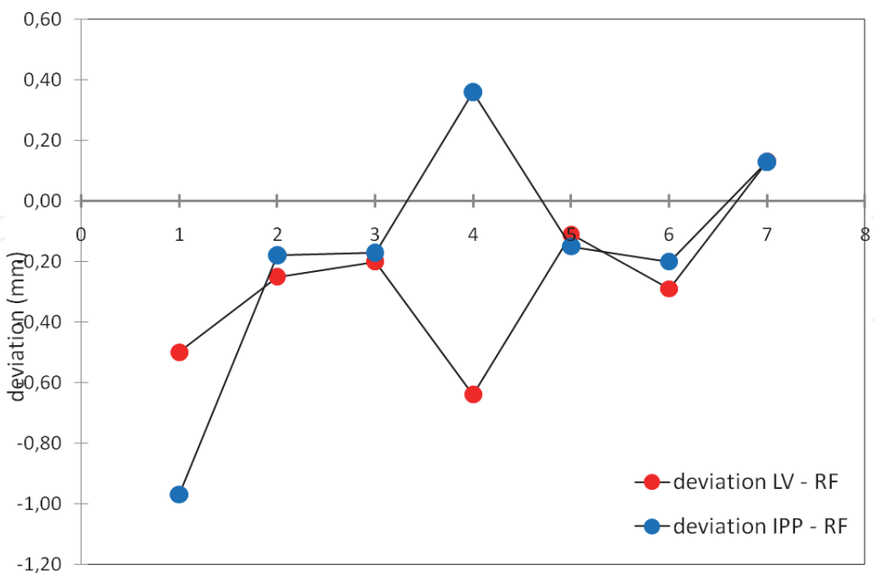

(b)

Fig. 11. CT slice thickness accuracy obtained for a 5 mm RF value: (a) sample set (blue: IPP; red: LV); (b) deviation from the RF value (blue: IPP; red: LV).

Finally, in Table 5, the results obtained by measuring the slice thickness accuracy by employing the IPP and the LV procedures are compared with the corresponding 2 mm RF value and mean values and standard deviation are also indicated. From the analysis of the data of Table 5, it can be observed that the mean value calculated by the LV dataset is significantly closer to the RF value than that calculated from the IPP dataset. This further supports the validity of the proposed technique.

RF Values (mm)	LV (mm)	LV mean value and standard deviation (mm)	IPP (mm)	IPP mean value and standard deviation (mm)
2	2.66	2.32±0.48	2.79	2.79±0.16
	3.00		2.75	
	2.06		2.83	
	1.96		2.56	
	1.95		3.00	

Table 5. Slice thickness accuracy results obtained with LV and IPP for a 2 mm RF value, using different types of CT scanners.

The data of Table 5 are represented in graphical form in Fig 12, where the slice thickness accuracy results obtained using IPP and LV (blue: IPP; red: LV) and their deviation from the 2 mm RF value (blue: IPP; red: LV) are presented.

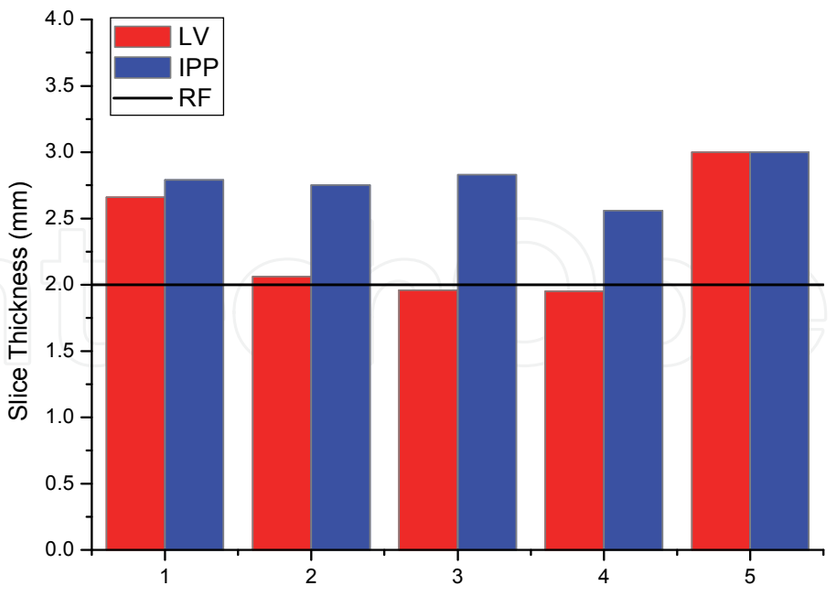

Fig. 12. (a)

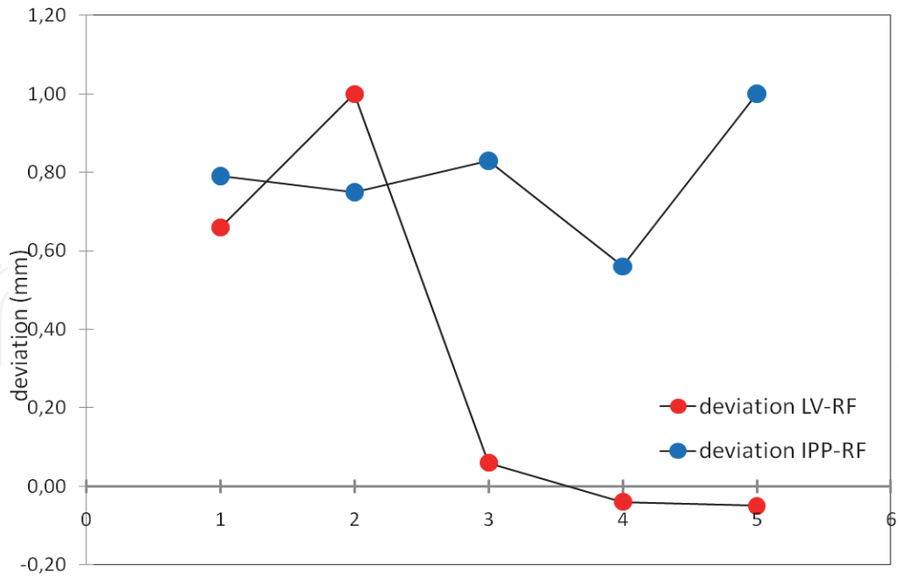

(b)

Fig. 12. CT slice thickness accuracy obtained for a 2 mm RF value: (a) sample set (blue: IPP; red: LV); (b) deviation from the RF value (blue: IPP; red: LV).

Statistical analysis conducted on the datasets shown in Tables 3-5 yielded the F-values reported in Table 6. Such F-values indicate that there is no significant statistical variation between the two different procedures, thus validating the methodology.

RF Values (mm)	F_C	F_T
10	0.011	4.54
5	0.332	4.67
2	4.18	5.12

Table 6. F values calculated for different RF values (F_C). These F-values were compared to the tabulated ones (F_T) for the P=0.05 confidence level.

3.2 MRI medical devices

Two-dimensional images of the wedge of the dedicated phantom were acquired using the Scan Head Protocol reported in Table 2. A typical MRI image of the PMMA box and the corresponding line profile calculated with the in-built MRI software are shown in Fig. 13. The preliminary results obtained using the IPP and LV procedures discussed above applied to MRI are reported in Table 7 for a RF value of 10 mm. In this case the slice thickness accuracy measured using an in-built MRI software (CS) is also included. The corresponding mean value and standard deviation of the three datasets are also reported.

Also in this case, the mean values calculated from the three different datasets of measurements are comparable between them. However, whereas the standard deviations obtained from CS and LV procedures are comparable, those obtained from IPP and LV are significantly different. The LV procedure provides a narrower deviation with respect to that obtained with IPP, which gives evidence for a more accurate measurement.

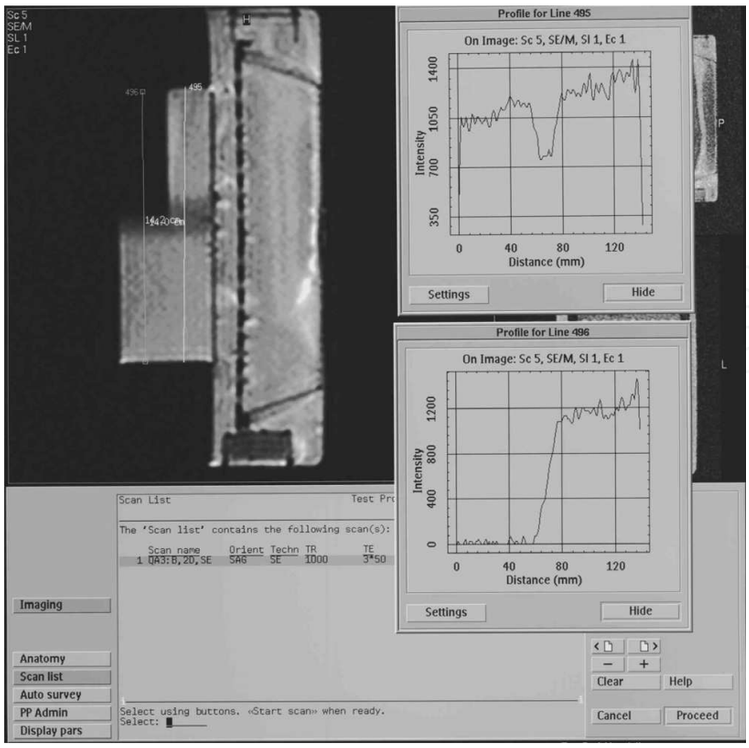

Fig. 13. MRI PMMA box image and corresponding line profile appearing on the MRI display. It is possible to notice the related line profile as obtained directly at the equipment console.

The slice thickness accuracy data of Table 7 are presented in graphical form in Fig. 14(a), where the slice thickness accuracy determined directly at the equipment console and that measured using the IPP and the LV procedures are compared. In Fig. 14(b) deviations from the RF value are presented for the three sets of data.

RF value (mm)	CS (mm)	CS mean value and standard deviation (mm)	LV (mm)	LV mean value and standard deviation (mm)	IPP (mm)	IPP mean value and standard deviation (mm)
10	10.1	10.05±0.17	10.3	10.05±0.15	9.80	9.96±0.31
	9.90		9.92		9.85	
	10.3		10.2		9.80	
	9.80		10.0		10.5	
	10.1		9.94		10.1	
	10.2		10.17		10.3	
	9.90		9.95		9.60	
	10.1		9.90		9.90	

Table 7. Comparison between the slice thickness accuracy obtained from the MRI in-built software (CS), the Image Pro Plus (IPP) procedure and the dedicated LabView (LV) software for a 10.0 mm Reference (RF) value. In the same table mean values and corresponding standard deviations for the three different procedures are also reported.

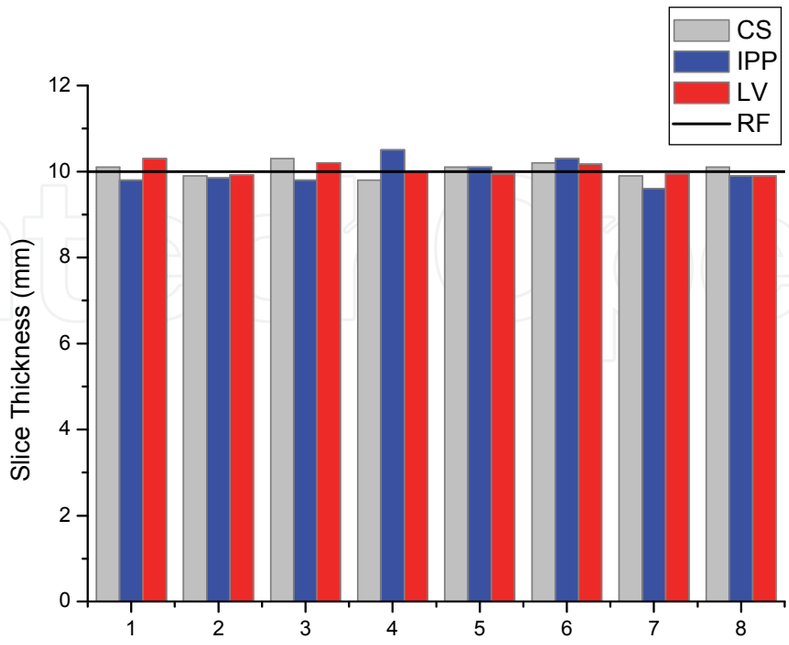

(a)

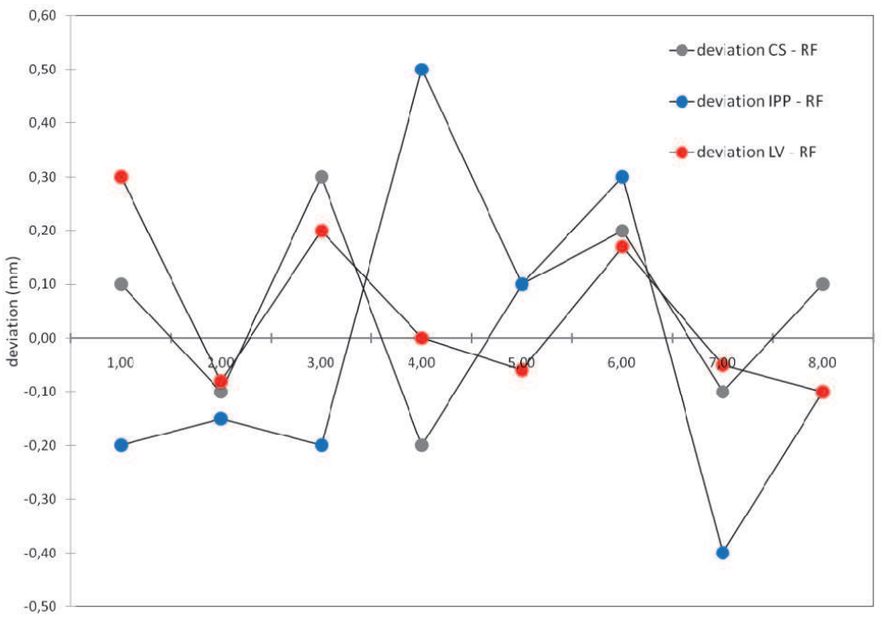

(b)

Fig. 14. MRI slice thickness accuracy obtained for a 10 mm RF value: (a) data obtained directly from the MRI scanner (CS) and measured using the IPP and the LV procedures (grey: CS; blue: IPP; red: LV); (b) deviation from the RF value (grey dots: CS; blue dots: IPP; red dots: LV).

The F-test is then used to verify that the three datasets are comparable (Table 8). As evident from the data of Table 8, the F values calculated for the three sets of data are significantly smaller than that tabulated (F_T) for a P=0.05 confidence level in all cases. Therefore, there is no significant statistical difference between the three different procedures, thus validating the novel LV procedure proposed here also for MRI imaging.

Datasets	F_C	F_T
CS-IPP	0.836	4.54
CS-LV	0.00165	
IPP-LV	0.513	

Table 8. Results of the F-test calculated comparing the CS, IPP and LV datasets (F_C). These F-values were compared to the tabulated ones (F_T) for the P=0.05 confidence level.

3.3 US scanners

The novel PMMA phantom proposed here (Fig. 7) was utilised also to test the elevation resolution in ultrasound systems. Preliminary measurements have been conducted on US probes to evaluate if it is possible to measure the beam width in the elevation plane. To correctly determine the elevation beam profile, it was necessary to slightly modify the phantom. In particular, the septum position was modified and, for the beam width evaluation, the inclined plane was oriented 28 degrees to the top and bottom surface, so the probe intersects the inclined plane at 28 degrees. The upper side of the inclined surface was filled with ultrasound gel, as conductive medium. The echoes reflected from the inclined plane are displayed as a horizontal band. Because the beam intersects the plane at 28 degrees, the beam width in the elevation plane can be calculated as follows:

$$ST = FWHM \cdot \tan(28°) \tag{5}$$

The above technique enables the measurement of the elevation dimension of the beam at a single depth only. To determine the entire profile in the elevation plane, the probe must be moved horizontally along the surface of the phantom to make a series of measurements, with the beam intersecting the inclined plane at different depths. With the use of the novel phantom described here, the resolution in the elevation plane is completely independent from the lateral resolution in the scanning plane. The new phantom proposed here is easy to use and does not require any additional equipment and the results are immediately displayed on the screen of the dedicated PC.

4. Conclusion

Slice thickness represents an important parameter to be monitored in CT, MRI an US. Partial volume effects can significantly alter sensitivity and specificity. Especially for MRI, quantitative measurements such as T_1 and T_2, are also greatly influenced by the accuracy of the slice thickness. Inaccuracies in the measurement of this parameter may result in inter-slice interference in multi-slice acquisitions, leading to invalid SNR measurements. In addition, for the US scanners, significant differences in image resolution can occur because of variations in the beam width of the elevation plane. So, it is important to know the profiles of the elevation planes of various probes to choose the probe that offers resolution

in the elevation plane that is most appropriate for the particular clinical application. Moreover, slice thickness accuracy is an important element also in the QC program for CT scanner, because quantitative CT analysis is heavily dependent on accuracy of slice thickness. Therefore, to provide an adaptable, reliable and robust procedure to evaluate the slice thickness accuracy a novel, dedicated phantom and corresponding LabView-based procedure have been proposed here, up to date applied to both CT and MRI devices. The new PMMA box proposed here to be associated with the dedicated software enables an innovative, accurate, easily applicable and automated determination of this parameter.

The carried on studies have utilised the 2 mm septum because the z axis dimensions for rotating anode x-ray tube foci are typically less than this value, but is our intention reduce the septum width, in order to evaluate the slice thickness also for the helicoidal CT scanners, that can reach slice widths smaller than 2 mm.

The accuracy (standard deviation) obtained with the novel procedure proposed here is significantly higher than that obtained with other procedures (e.g., in-built software, IPP).

This new slice thickness accuracy procedure is proposed as an alternative to the commonly adopted ones, which are typically complicated by the use of ad-hoc software and phantoms distributed by manufacturers and specific to the medical equipment. The proposed method employs a novel universal phantom, coupled with a dedicated LabView-based software that can be used on any CT and MRI scanner in a quick, simple and reproducible manner.

The readiness and applicability of the proposed procedure has been validated by quantitative tests using several different medical devices and procedures. In all cases the results obtained using the novel proposed procedure were statistically compatible with other commonly used procedures, but provided a very immediate determination of the slice thickness for both CT and MRI equipments, thus confirming the flexibility of the described method, its simplicity and reproducibility as an efficient tool for quick inspections.

The same procedure should be suitable also for determining elevation accuracy on US scanner: in fact, preliminary results confirmed that the novel phantom, opportunely modified, when coupled with the LabView dedicated software, allowed measurements of the section thickness

5. References

CEI EN 61223-2-6. (1997). Evaluation and routine testing in medical imaging departments. Part 2-6: Constancy tests – X-ray equipments for computed tomography. CEI, (Ed.), pp. 1-26

Chen, C.C.; Wan, Y.L.; Wai, Y.Y. & Liu, H.L. (2004). Quality assurance of clinical MRI scanners using ACR MRI phantom: preliminary results. *Journal of Digital Imaging,* Vol. 17, No. 4 (December 2004), pp. 279-284, ISSN 0897-1889

General Electric Medical System. (2000). Quality Assurance. In: *CT HiSpeed DX/i Operator manual Rev. 0*. General Electric Company (Ed.). Chapter 6, pp. 1-28

Goodsitt, M.M.; Carson, P.L.; Witt, S.; Hykes, D.L. & Kofler, J.M. (1998). Real-time B-mode ultrasound quality control test procedures. Report of the AAPM ultrasound task group No. 1. *Medical Physics,* Vol. 25, No. 8 (August 1998), pp. 1385-1406, ISSN 0094-2405

Judy, P.F.; Balter, S.; Bassano, D.; McCollough, E.C.; Payne, J.T. & Rothenberg, L. (1977). Phantoms for performance evaluation and quality assurance of CT scanners.

AAPM Report No. 1 (American Association of Physicist in Medicine, Chicago, Illinois, 1977)

Lerski R.A. & Mc Robbie D.W. (1992). EUROSPIN II. Magnetic resonance quality assessment test objects. Instruction for use. Diagnostic Sonar LTD (January 1992), pp. 1-79

Markowski, C.A. & Markowski, E.P. (1990). Conditions for the effectiveness of a preliminary test of variance. *The American Statistician,* Vol. 44, No. 4 (November 1990), pp. 322-326, ISSN 0003-1305

Mc Robbie, D.W.; Lerski, R.A.; Straughan, K.; Quilter, P. & Orr, J.S. (1986). Investigation of slice characteristics in nuclear magnetic resonance imaging. *Physics in Medicine and Biology,* Vol. 31, No. 6 (June 1986), pp. 613-626, ISSN 0031-9155

Mutic, S.; Palta, J.R.; Butker, E.K.; Das, I.J.; Huq, M.S.; Loo, L.N.D.; Salter, B.J.; McCollough, C.H. & Van Dyk, J. (2003). Quality assurance for computed-tomography simulators and the computed tomography simulation process. Report of the AAPM radiation therapy committee task group No. 66. *Medical Physics*, Vol. 30, No. 10 (October 2003), pp. 2762-2792, ISSN 0094-2405

Narayan, P.; Suri, S.; Choudhary, S.R. & Kalra, N. (2005). Evaluation of Slice Thickness and Inter Slice Distance in MR scanning using designed test tool. *Indian Journal of Radiology & Imaging,* Vol. 15, No. 1 (February 2005), pp.103-106, ISSN 0971-3026

National Instruments. (2001). LabView User Manual. National Instruments Corporation (Ed.). Available from http://www.ni.com/pdf/manuals/320999d.pdf

Och, J.G.; Clarke, G.D.; Sobol, W.T.; Rosen, C.W. & Ki Mun, S. (1992). Acceptance testing of magnetic resonance imaging systems: Report of AAPM Nuclear Magnetic Resonance Task Group No.6. *Medical Physics,* Vol. 19, No. 1 (January-February 1992), pp. 217-229, ISSN 0094-2405

Philips. (1997). Performance Phantom C instruction manual. In: Tomoscan CX/Q technical documents. pp. 1-18

Price, R.R.; Axel, L.; Morgan, T.; Newman, R.; Perman, W.; Schneiders, N.; Selikson, M.; Wood, M. & Thomas S.R. (1990). Quality assurance methods and phantoms for Magnetic Resonance Imaging. Report of the AAPM Nuclear Magnetic Resonance Task Group No. 28. *Medical Physics,* Vol. 17, No. 2 (March-April 1990), pp. 287-295, ISSN 0094-2405

Rampado, O.; Isoardi, P. & Ropolo, R. (2006). Quantitative assessment of computed radiography quality control parameters. *Physics in Medicine and Biology,* Vol. 51, No. 6 (March 2006), pp. 1577-1593, ISSN 0031-9155

Rehani, M.M.; Bongartz, G.; Golding, S.J.; Gordon, L.; Kalender, W.; Albrecht, R.; Wei, K.; Murakami, T. & Shrimpton, P. (2000). Managing patient dose in computed tomography. *Annals of ICRP*, Vol. 30, No. 4 (December 2000), pp. 7-45, ISSN 0146-6453

Richard, B. (1999). Test object for measurement of section thickness at US. *Radiology,* Vol. 211, No. 1 (April 1999), pp. 279-282, ISSN 0033-8419

Sansotta, C.; Testagrossa, B.; de Leonardis, R.; Tripepi, M.G. & Vermiglio, G. (2002). Remote image quality and validation on radiographic films. *Proceedings of the 7th Internet World Congress for Biomedical Sciences, INABIS 2002,* Available from http://www.informedicajournal.org/a1n2/files/papers_inabis/sansotta1.pdf

Skolnick, M.L. (1991). Estimation of Ultrasound beam width in the elevation (section thickness) plane. *Radiology,* Vol. 180, No. 1 (July 1991), pp. 286-288, ISSN 0033-8419

Torfeh, T.; Beaumont, S.; Guédon, J.P.; Normand, N. & Denis, E. (2007). Software tools dedicated for an automatic analysis of the CT scanner Quality Control's Images, In: *Medical Imaging 2007: Physics of Medical Imaging. Proceedings of SPIE*, Vol. 6510, J. Hsien & M.J. Flynn (Eds.), 65104G, ISBN 978-081-9466-28-0, San Diego, California, USA, March 6, 2007

Testagrossa, B.; Novario, R.; Sansotta, C.; Tripepi, M.G.; Acri, G. & Vermiglio, G. (2006). Fantocci multiuso per i controlli di qualità in diagnostica per immagini. *Proceedings of the XXXIIIth International Radio Protection Association (IRPA) Conference,* IRPA, ISBN 88-88648-05-4, Turin, Italy, september 20-23, 2006

Vermiglio, G.; Testagrossa, B.; Sansotta, C. & Tripepi, M.G. (2006). Radiation protection of patients and quality controls in teleradiology. *Proceedings of the 2nd European Congress on Radiation Protection «Radiation protection: from knowledge to action».* Paris, France, May 15-19, 2006, Available from http://www.colloquium.fr/06IRPA/CDROM/docs/P-121.pdf

Vermiglio, G.; Tripepi, M.G.; Testagrossa, B.; Acri, G.; Campanella, F. & Bramanti, P. (2008). LabView employment to determine dB/dt in Magnetic Resonance quality controls. *Proceedings of the 2nd NIDays,* pp. 223-224. Rome, Italy, February 27, 2008

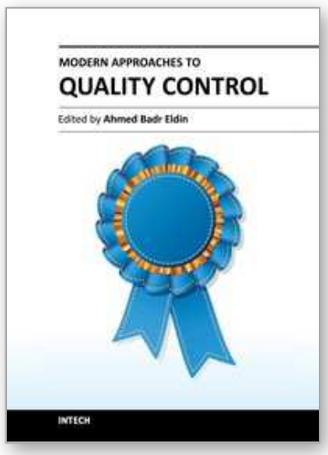

Modern Approaches To Quality Control

Edited by Dr. Ahmed Badr Eldin

ISBN 978-953-307-971-4
Hard cover, 538 pages
Publisher InTech
Published online 09, November, 2011
Published in print edition November, 2011

Rapid advance have been made in the last decade in the quality control procedures and techniques, most of the existing books try to cover specific techniques with all of their details. The aim of this book is to demonstrate quality control processes in a variety of areas, ranging from pharmaceutical and medical fields to construction engineering and data quality. A wide range of techniques and procedures have been covered.

How to reference

In order to correctly reference this scholarly work, feel free to copy and paste the following:

Giuseppe Vermiglio, Giuseppe Acri, Barbara Testagrossa, Federica Causa and Maria Giulia Tripepi (2011). Procedures for Evaluation of Slice Thickness in Medical Imaging Systems, Modern Approaches To Quality Control, Dr. Ahmed Badr Eldin (Ed.), ISBN: 978-953-307-971-4, InTech, Available from: http://www.intechopen.com/books/modern-approaches-to-quality-control/procedures-for-evaluation-of-slice-thickness-in-medical-imaging-systems

INTECH
open science | open minds

InTech Europe
University Campus STeP Ri
Slavka Krautzeka 83/A
51000 Rijeka, Croatia
Phone: +385 (51) 770 447
Fax: +385 (51) 686 166
www.intechopen.com

InTech China
Unit 405, Office Block, Hotel Equatorial Shanghai
No.65, Yan An Road (West), Shanghai, 200040, China
中国上海市延安西路65号上海国际贵都大饭店办公楼405单元
Phone: +86-21-62489820
Fax: +86-21-62489821

IntechOpen